buildings

MDPI

Article

Numerical Investigation on Auxiliary Heat Sources for Horizontal Ground Heat Exchangers

Alexandru-Mihai Bulmez *, Vasile Ciofoaia, Gabriel Năstase, George Dragomir, Alin-Ionuț Brezeanu, Nicolae-Fani Iordan, Sorin-Ionuț Bolocan, Mariana Fratu, Costel Plești, Christiana Emilia Cazacu and Ovidiu Deaconu

Department of Building Services, Faculty of Civil Engineering, Transilvania University of Brasov, 500152 Brasov, Romania

* Correspondence: alexandru.bulmez@unitbv.ro

Abstract: Human interference with the Earth's climate cannot be ignored any longer. Renewable energy sources need utmost attention in all energy sectors. For buildings, geothermal energy for heating, cooling, and domestic hot water is a sustainable solution. Horizontal ground heat exchangers (HGHE) demonstrate promising results with low installation costs. Research is focused on increasing their thermal performances by structural improvements and ground thermal proprieties improvements, with little research on using auxiliary heat to increase their performances. A numerical model for an HGHE was established to investigate the effects of auxiliary heat sources on the performances of the HGHE. The results demonstrate that heat transfer into the HGHE increases the overall ground temperature at the end of the heating season by 138.50% compared with no heat transfer from auxiliary heat sources. The ground freezing period decreased by approximately 24.74% by having a heated basement, approximately 40.20% by transferring heat with solar thermal panels, and approximately 62.88% by using both auxiliary heat sources. The difference between the undisturbed ground temperature and the ground temperature with no auxiliary heat sources at the end of the season was 3.45 °C. The difference between the undisturbed ground temperature and the ground temperature with all auxiliary heat sources resulted in 0.92 °C.

Keywords: horizontal ground heat exchanger; auxiliary heat source; heated basement; solar thermal panel; ground freezing period; ground temperature

Citation: Bulmez, A.-M.; Ciofoaia, V.; Năstase, G.; Dragomir, G.; Brezeanu, A.-I.; Iordan, N.-F.; Bolocan, S.-I.; Fratu, M.; Plești, C.; Cazacu, C.E.; et al. Numerical Investigation on Auxiliary Heat Sources for Horizontal Ground Heat Exchangers. *Buildings* **2022**, *12*, 1259. https://doi.org/10.3390/buildings12081259

Academic Editors: Benedetto Nastasi and Giovanni Pernigotto

Received: 7 July 2022
Accepted: 16 August 2022
Published: 17 August 2022

1. Introduction

Anthropogenic interference with the Earth's climate since the Industrial Revolution has been done unknowingly until several decades ago. Today, it is estimated that all fossil fuels must be replaced over the next 30 years [1], with the purpose of stopping the mean global temperature rise at values under 2 °C until 2036 [2]. Recent studies show that global total excess mortality caused by air pollution due to fossil fuels reached 8.79 million per year, with a 95% confidence interval and that the global mean loss of life expectancy is 2.9 years per year [3].

Air pollution due to fossil fuel emissions released into Earth's atmosphere is anthropogenically caused by agriculture and forestry, industry, power generation, traffic, and energy used in buildings, commercials, or residential. Furthermore, world energy demand is rising due to population growth and technological and economic human advances [4]. In developed countries, of the total energy consumption, 20–40% accounts for the energy used in buildings [5]. Today there is an immense urge to tap into renewable energy sources. Geothermal renewable energy has special attention due to its sustainability for buildings heating, cooling, and domestic hot water production.

Heat pump systems are needed to tap into geothermal energy. For this, ground heat exchangers (GHE) are used. There are two general types of GHEs that are used: vertical

ground heat exchangers (VGHE) and horizontal ground heat exchangers. While VGHEs are 70–130 m [6] deep vertical boreholes, HGHEs are generally horizontal pipes at the ground surface between 1–3 m [7] deep. VGHEs are more efficient and use less land, but the installation cost is a lot higher compared to HGHEs [8]. HGHEs, on the other hand, are cheaper to install, but their efficiency is not as high as VGHEs, and they use more land space [9].

Considering this, plenty of research has been made recently on multiple solutions to increase the performance of HGHEs. Experimental and numerical studies have shown that the thermal performances depend on the daily and seasonal temperature variation at the ground surface, where the HGHEs are positioned [10]. Soil thermal proprieties and compaction levels also influence the thermal performances, as shown in [11]. Other solutions for increasing the thermal performances of HGHEs that were researched focused on the type of pipe arrangement, from simple U type to slinky or helical configurations, vertically or horizontally positioned [5,12–20]. Other studies focused on different types of HGHEs, such as a flat panel HGHE [7], resulting in the highest heat transfer rate per unit of land area among all configurations of HGHEs.

In [21], the authors researched an HGHE placed in the tunnel lining to investigate the thermal performance showing that groundwater flow has a considerable higher influence than tunnel ventilation on the heat pump efficiency. Moreover, other authors proposed configurations for pipes embedded in diaphragm walls [22] or the building foundation [23,24], showing that there is potential for such configurations, but they are highly dependent on conditions related to building destination, basement, and level of thermal insulation of the foundation. Another study [25] researched the thermal performances of energy piles HGHE as another way to increase the thermal performances and reduce the total space needed for HGHEs. Generally, HGHEs are water-ground heat exchangers. There are also HGHEs that are air-ground heat exchangers and are called horizontal air-ground heat exchangers (HAGHE). Although there is little research on them [26–31], lately, they have begun to receive more attention.

When designing an HGHE, it is of utmost importance to analyze the ground proprieties and the temperature variation where the HGHE will be positioned. Few studies [32,33] researched the heat balance and the ground temperature with the purpose of determining a necessary temperature threshold. Maintaining a heat balance and a certain ground temperature increases the performance of the heat pump for heating and cooling.

This work's purpose is to research alternative solutions to maintain a higher ground temperature inside the HGHE using auxiliary heat sources that transfer heat into the HGHE. For this, the placement in the proximity of a heated basement and the use of solar thermal panels to transfer heat inside the ground during the heat pump downtime were considered. In consequence, the secondary purpose is to study the effects of auxiliary heat transfer into the HGHE on the ground freezing period. This study considered the climate of Eastern Europe for the city of Brașov, Romania. Only the heating season was considered because the cooling loads are lower than the heating loads for this climate.

2. Numerical Method

2.1. Geometric Model

A numerical model was established using the finite element program COMSOL Multiphysics V5.5. The heat transfer consists of convective heat transfer of the fluid inside the pipe, convective heat transfer at the ground surface, radiative heat transfer at the ground surface, and conduction in the solid composite ground. To reduce the computational time and requirements, the following assumptions have been chosen:

- the system is simulated for the heating season;
- the ground is considered homogenous with constant thermos-physical proprieties;
- the HGHE pipes are considered one-dimensional lines with heat flux input;
- the surface heat transfer is approximated into mean temperatures of the exterior air;
- the heat transfer solved with COMSOL Multiphysics is only for solids.

Figure 1 illustrates the geometric model used for the numerical simulation. The HGHE is placed on purpose adjacent to the building basement wall, with the objective to use the residual heat lost from the basement. The overall area of the HGHE, where the pipe is buried, is approximately 25 m^2. The considered dimensions for simulation of the HGHE are 9 m length, 6 m width, 3 m depth, and 2 m width stretching inside the basement. The pipe is a Ø20 mm polyethylene pipe buried 1.2 m deep, in a simple U configuration, with a 50 cm step. The distance of the pipe from the basement wall is 1 m.

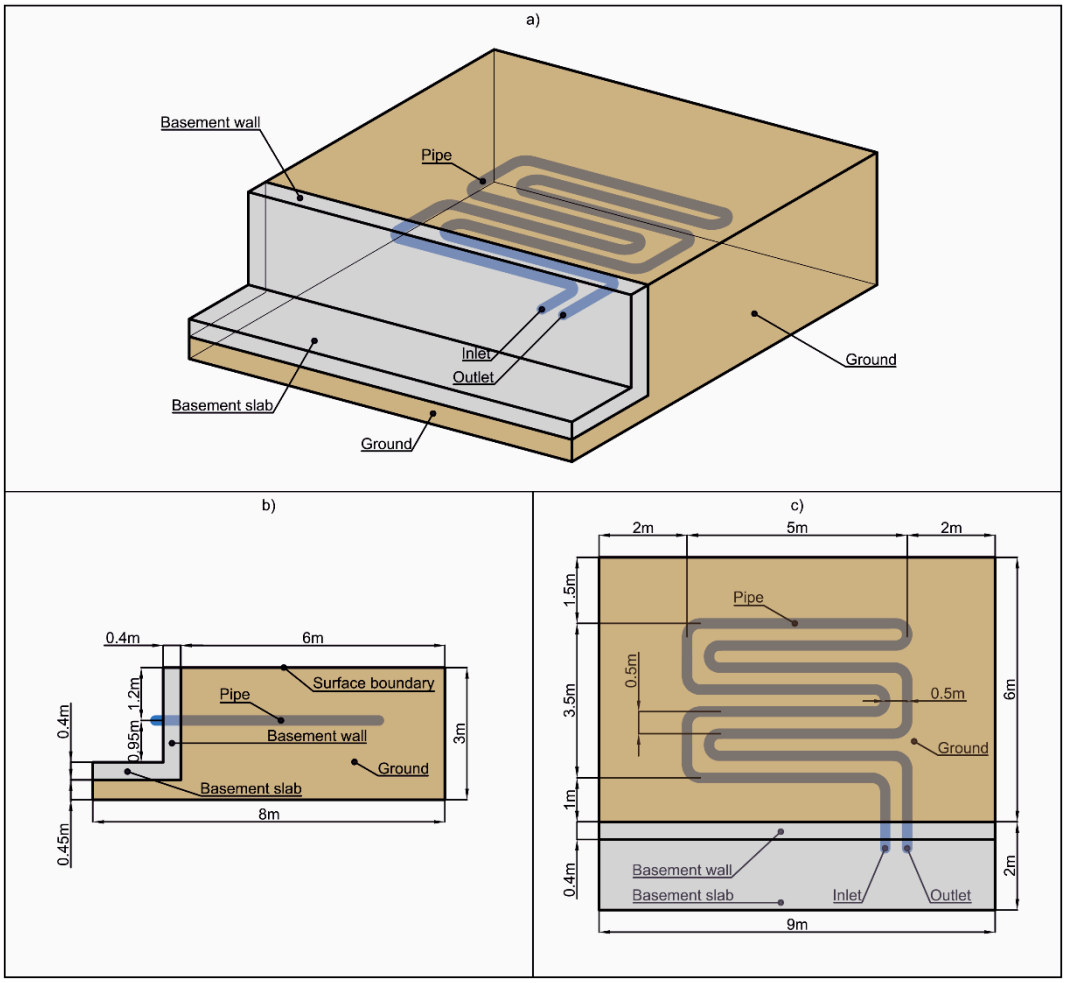

Figure 1. Geometrical model for the HGHE used for numerical simulation: (**a**) tri-dimensional view; (**b**) bi-dimensional side view; (**c**) bi-dimensional top view.

For simulation, the heat transfer for the solids module was used in the finite element software COMSOL Multiphysics V5.5. The purpose was to keep the computational cost at reasonable levels and maintain an accuracy level as high as possible. For that, a computational grid using the mesh coarsening factor of the finer (7 out of 9 factors) was used for the area surrounding the pipes and a mesh coarsening factor of fine (6 out of 9 factors) was used for the rest of the geometrical model, as illustrated in Figure 2. The element type used is a free tetrahedral for the entire geometry, as illustrated in Figure 2. In total, a number of 39,330 free tetrahedral elements were generated, with 466 edge elements and 2918 triangular elements. The smallest element alongside the pipes has a size of 36 mm and the biggest one, 495 mm, is in the farthest area from the basement and the pipes. The entire volume of the geometrical model is 187.1 m^3. With this setup, the computational time varied between 16 and 17 h. The time step was set up at a 2 h interval for a total of 181 days, corresponding to the entire heating season, starting from mid-October to mid-April.

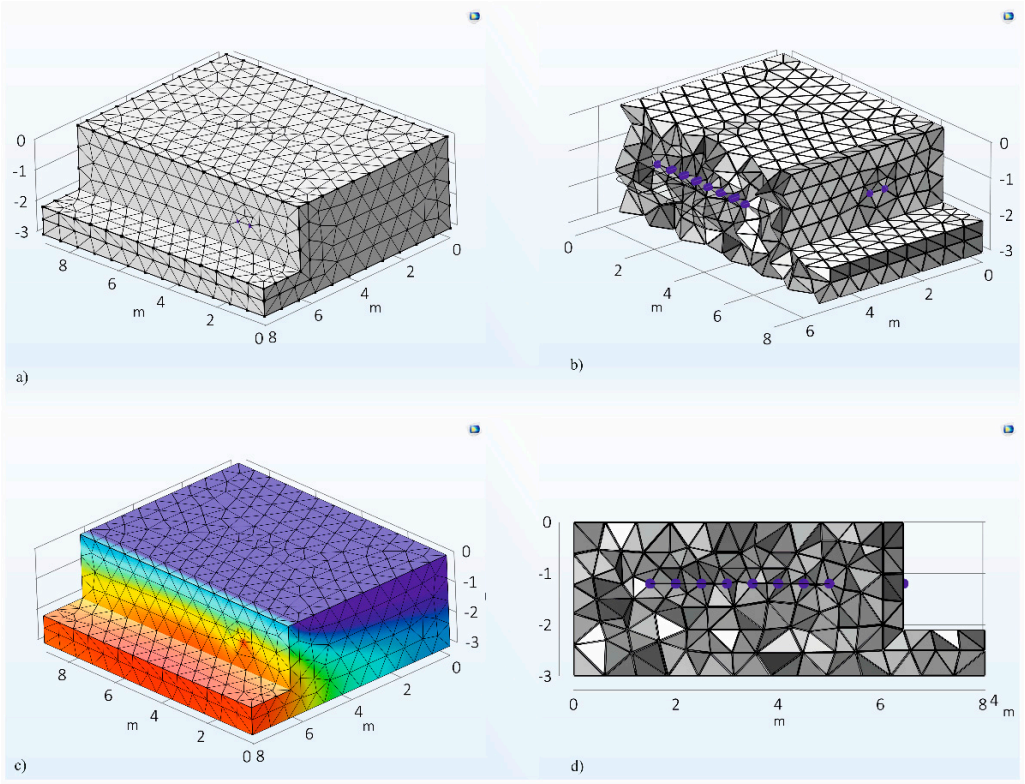

Figure 2. The tri-dimensional computational grid for the HGHE used for numerical simulation: (**a**) 3D computational grid exterior surfaces; (**b**) 3D section computational grid with interior and pipes visible; (**c**) 3D computational grid with temperature distribution; (**d**) 2D section perpendicular to the basement wall with pipes visible.

The thermal physics proprieties of the materials used for the simulation are presented in Table 1. The geometric model consists of three domains: the soil domain, the basement concrete wall/slab domain, and the polyethylene pipe domain.

Table 1. Model parameters.

Material	Parameter	Value	Unit
Soil	Density	1742	kg/m^3
	Thermal conductivity	1.5	W/m·K
	Specific heat capacity	1175	J/kg·K
Basement wall/slab	Density	2300	kg/m^3
	Thermal conductivity	1.8	W/m·K
	Specific heat capacity	880	J/kg·K
Polyethylene pipe	Pipe length	50	m
	Pipe step	50	cm
	Pipe depth	1.2	m
	Outer diameter	20	mm
	Thermal conductivity	0.4	W/m·K

The governing equation for solving tri-dimensional heat conduction is

$$\rho C_p \left(\frac{\partial T}{\partial t} + u_{trans} \nabla T \right) + \nabla (q + q_r) = -\alpha T : \frac{dS}{dt} + Q, \quad (1)$$

where ρ is the density (kg/m^3), Cp is the specific heat capacity at constant stress (J/(kg·K)), T is the absolute temperature (K), u_{trans} is the velocity vector of translational motion (m/s),

q is the heat flux by conduction (W/m^2), q_r is the heat flux by radiation (W/m^2), α is the coefficient of thermal expansion (1/K), S is the second Piola-Kirchhoff stress tensor (Pa), Q contains additional heat sources (W/m^3).

The term on the right-hand side of Equation (1) represents the thermoelastic damping effects in solids:

$$Q_{ted} = -\alpha T : \frac{dS}{dt}, \tag{2}$$

where the d/dt operator represents the material derivative which accounts for time steps, material, and spatial frames, as follows:

$$\frac{d}{dt} = \frac{\partial}{\partial t} + u_{(x,y,z)} \cdot \nabla_{(x,y,z)}, \tag{3}$$

in which the term $u \cdot \nabla$ accounts for the quantity of heat transferred by convection by translational motion, and x,y,z represents the coordinates for which the position vectors (X,Y,Z) are solved. The relation between the coordinates and the position vectors is characterized by the deformation gradient:

$$F = \begin{bmatrix} \frac{\partial x}{\partial X} & \frac{\partial x}{\partial Y} & \frac{\partial x}{\partial Z} \\ \frac{\partial y}{\partial X} & \frac{\partial y}{\partial Y} & \frac{\partial y}{\partial Z} \\ \frac{\partial z}{\partial X} & \frac{\partial z}{\partial Y} & \frac{\partial z}{\partial Z} \end{bmatrix}, \tag{4}$$

which accounts for distances dx and dX in the material and spatial frames according to:

$$dx = FdX, \tag{5}$$

The volume ratio field is the determinant of the deformation gradient, det(F). The deformation gradient tensor and its determinant are needed for the computational software in the conversion of physical quantities between material and spatial frames.

2.2. Initial and Boundary Conditions

The initial ground temperature corresponds to the undisturbed ground temperature at the start of the season. The boundary conditions established in the numerical model are presented in Table 2 and were set according to the best practice guidelines [7,10]. The exterior temperature was set as a Dirichlet boundary condition for the exterior ground surface. The temperature input was set every 2 h for 181 days. The bottom ground surface is affected by the inward heat flux from the earth's interior [32]. A Neumann heat flux boundary condition was set for it, with the value of 0.045 W/m^2, corresponding to the geothermal gradient of 0.03 K/m and ground thermal conductivity of 1.5 W/m·K [32]. From the basement, heat is transferred toward the HGHE all the time because the temperature inside is always higher than the temperature in the HGHE. Thus, a Neumann heat flux boundary condition was set for the basement wall and slab. The heat flux corresponds to the interior temperature of the basement for each case simulated. The boundary condition used for the pipe is a Neumann condition. Heat flux is transferred inward and outward of the HGHE, corresponding to the heat extracted and transferred with the thermal solar panels according to the measurements registered on-site.

Table 2. Boundary conditions.

Location on Geometric Model	Boundary Condition Type
Exterior ground surface	Temperature
Bottom ground surface	Heat flux
Basement wall/slab surface	Heat flux
Pipe	Heat flux
All other surfaces	Periodic

At the surfaces where domains overlap, continuity boundary conditions are set automatically by COMSOL Multiphysics. The software allows the possibility to change that option, but, in this case, a continuity boundary condition between pipes, soil, and concrete was needed. The continuity boundary condition solves the heat transfer between solids according to thermodynamic laws.

2.3. Validation of the Numerical Model

The numerical model established in this study is based on an experimental HGHE that was thoroughly described in a previous paper [34]. The comparative analysis with on-site experimental data validated the numerical model. Due to the high variation of the temperature at the ground surface where HGHEs are positioned, this model was found to be time step and grid independent. Data registered on site was used for simulation purposes. Exterior temperature, extracted heat from HGHE, and heat transferred into HGHEs were used.

3. Results

Horizontal ground heat exchanger efficiency is highly dependent on outside temperature variation; because of this, it is not as reliable as the vertical ground heat exchanger. The main purpose of this study is to reduce the ground temperature variation during the heating season by using auxiliary heat sources to stabilize the ground temperature. With the data from the experimental site [34], the following cases were simulated:

- Case 1: HGHE with no auxiliary heat sources;
- Case 2: HGHE with heated basement;
- Case 3: HGHE with heat from solar thermal panels;
- Case 4: HGHE with heat from the heated basement and solar thermal panels combined.

To observe the auxiliary heat impact on the ground temperature inside the HGHE, the following parameters registered on-site were used in all four numerical studies:

- Exterior temperature;
- Heat extracted and transferred inside the HGHE;
- All physical geometry-related parameters.

3.1. Case 1: HGHE with No Auxiliary Heat Sources

For the first numerical study, no auxiliary heat source was considered. The temperature in the basement was set at 10 °C, in accordance with the temperature of an unheated basement, for the entire simulation period. At 10 °C, the unheated basement temperature is higher than the ground temperature where HGHE is positioned and it works as a heat source. It was considered as such because the simulation replicated the experimental HGHE position. Besides that, it was considered a common placement for HGHEs.

Figure 3 illustrates tri-dimensional temperature gradients for six days, representing the middle of each month of the heating season, starting with mid-November and ending with mid-April. After mid-November, the temperature inside the HGHE, at pipe depth, decreases below the freezing point due to exterior temperature decrease cumulated with heat extraction from the ground. The freezing period continues for approximately three months and the mean ground temperature increases above the freezing point after mid-February.

At season peaks, the lowest temperatures are visible, and the ground froze for depths below the pipe depth, which is also a common occurrence for HGHEs. The proximity to the unheated basement has clearly an influence. The higher the temperature difference between the temperature inside the basement and the temperature inside the HGHE, the more pronounced the heat transfer is. Up to 2.5 to 3 m, the ground temperature is influenced by the basement temperature. At the end of the heating season, in mid-April, the ground temperature at the surface reaches the values of the unheated basement and the temperature inside the HGHE is lower due to heat depletion during the heating season.

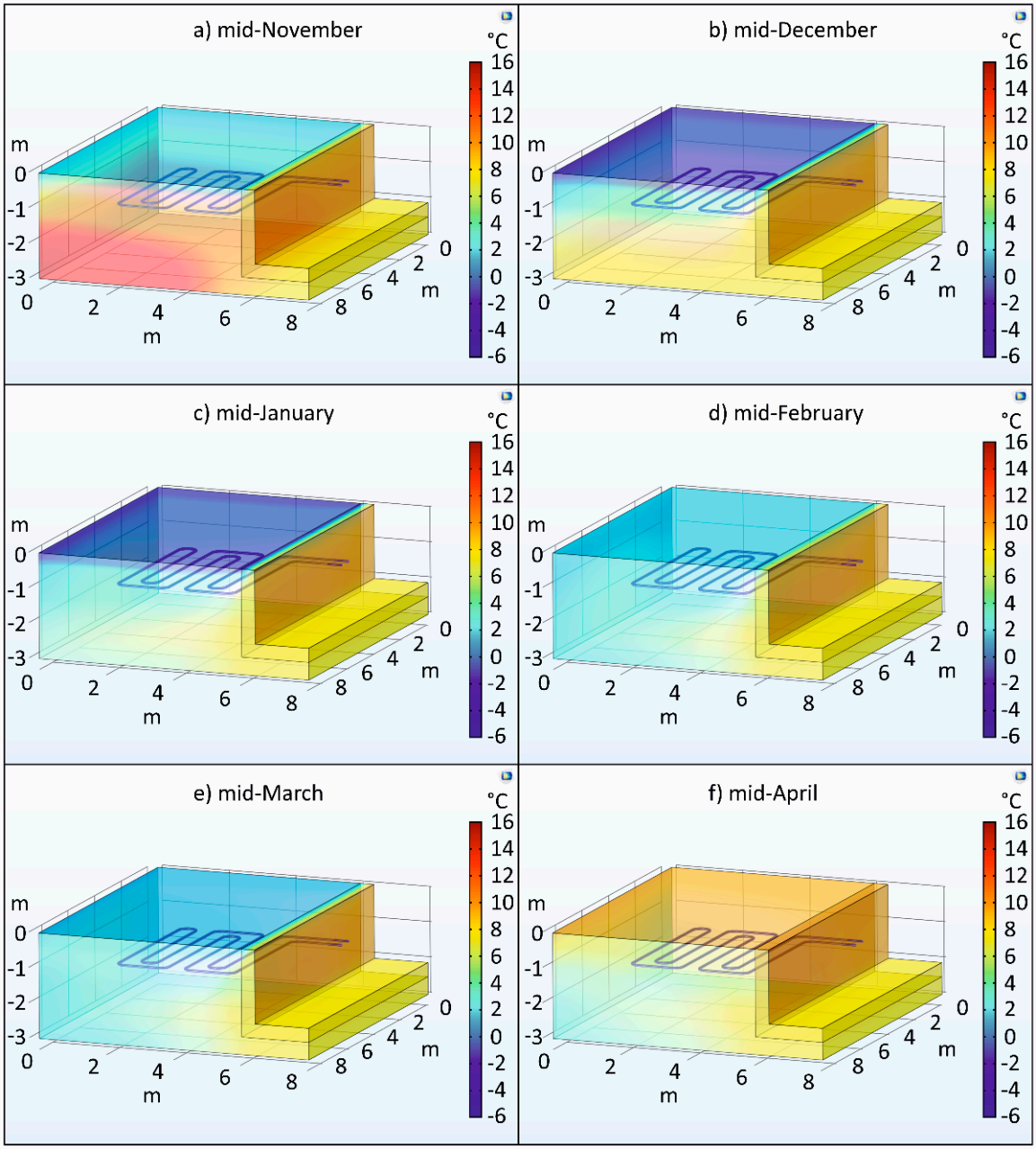

Figure 3. The tri-dimensional temperature gradients for the simulation case 1—HGHE with no auxiliary heat sources: (**a**) mid-November; (**b**) mid-December; (**c**) mid-January; (**d**) mid-February; (**e**) mid-March; (**f**) mid-April.

Figure 4 consequently illustrated tri-dimensional temperature isosurfaces for the same six days illustrated in Figure 3. The temperature layers visible in Figure 4 indicate that the ground is uniformly affected by the exterior temperature. The unheated basement represents the area with the highest temperature, thus working as a heat source for the HGHE, as Figure 3 also illustrates. The results illustrated in Figures 3 and 4 indicate when the temperature at pipe depth has values close to the undisturbed ground temperature, and the temperature layers are uniform in correlation with depth. When the reverse is occurring, uniformity in correlation with depth is not occurring, and the effects from the basement can be observed.

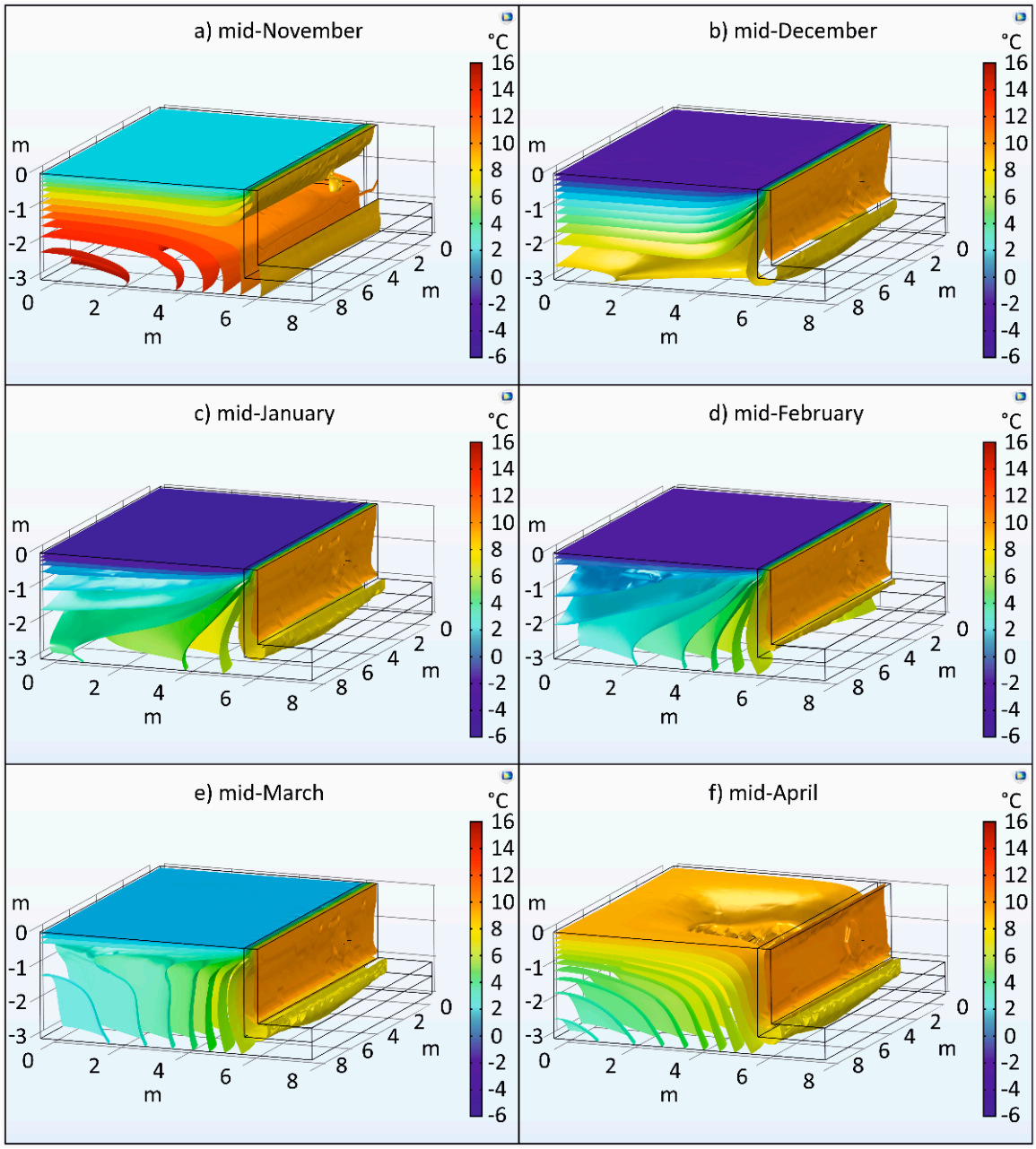

Figure 4. The tri-dimensional temperature isosurfaces for the simulation case 1—HGHE with no auxiliary heat sources: (**a**) mid-November; (**b**) mid-December; (**c**) mid-January; (**d**) mid-February; (**e**) mid-March; (**f**) mid-April.

Simulation case 1, represents a common application for residential buildings. Although, in some applications, the building does not have a basement, or the placement is farther away from the building. The results, in this case, illustrate how ground temperature distribution varies inside the HGHE for common applications in the present day. Generally, the ground freezes at pipe depth and measures are considered, such as avoiding the areas where sewerage and water pipes are present and using a solution of water with ethylene glycol as a thermal agent for the HGHE pipe circuit.

3.2. Case 2: HGHE Heated Basement

The second simulation case considered the basement as heated and the temperature was increased to 18–20 °C. The basement wall and slab were considered uninsulated for comparison purposes because the experimental conditions [34] were the same. Although

the temperature at the basement wall is higher by a few degrees, it can be observed in Figure 5 that the overall temperature inside the HGHE increased. This occurs because heat is being transferred from the basement to the surrounding ground, where the HGHE is positioned at higher quantities as a result of an increased temperature difference between basement and ground temperatures. Thus, the overall temperature inside the HGHE at pipe depth increased by approximately 1.5–2 °C.

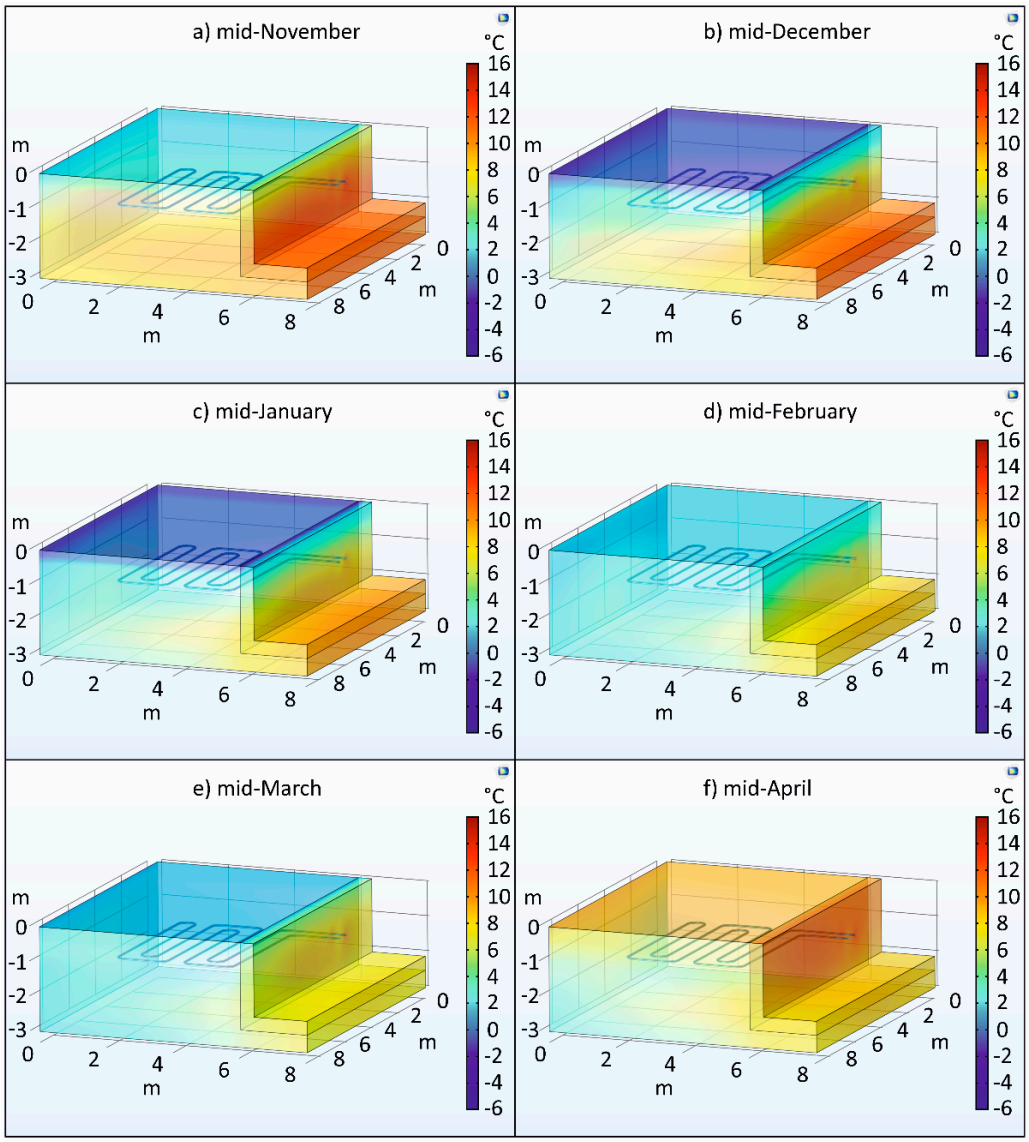

Figure 5. The tri-dimensional temperature gradients for the simulation case 2—HGHE with a heated basement: (**a**) mid-November; (**b**) mid-December; (**c**) mid-January; (**d**) mid-February; (**e**) mid-March; (**f**) mid-April.

Although the temperature inside the ground at the heating season start is the same as in simulation case 1, at the end of the heating season, the temperature inside the ground is higher when Figures 3 and 5 are observed. This indicates the positive effect the heated basement had on increasing the overall ground temperature. Similarly, the lowest temperature at the season peak is higher than the temperature from simulation case 1, also indicating that the heated basement contributed to maintaining a higher temperature inside the HGHE.

Compared with results from simulation case 1, the temperature alongside the height of the basement wall is higher at the bottom and lower at the upper part. This indicates that

there is a more pronounced heat transfer due to the higher temperature difference between the basement interior and ground temperature. Up to mid-February, this effect is visible and it indicates that although the heat was transferred into the HGHE, a part of that heat is lost to the exterior air near the building wall.

In concordance with Figure 5, Figure 6 also illustrates a more pronounced heat transfer from inside the basement towards the exterior ground and exterior air. It can be observed that the season peak benefited the most from heat transfer from the heated basement. This occurs due to the higher temperature difference between the ground and the heated basement in that period, indicating that the heat transfer was intensified; thus, a higher quantity of heat was transferred into the HGHE. In Figure 6, the non-uniformity of heat distribution layers with depth is observed. This occurs due to the high-temperature difference between the basement and the ground and it denotes the intensified heat transfer, as previously mentioned.

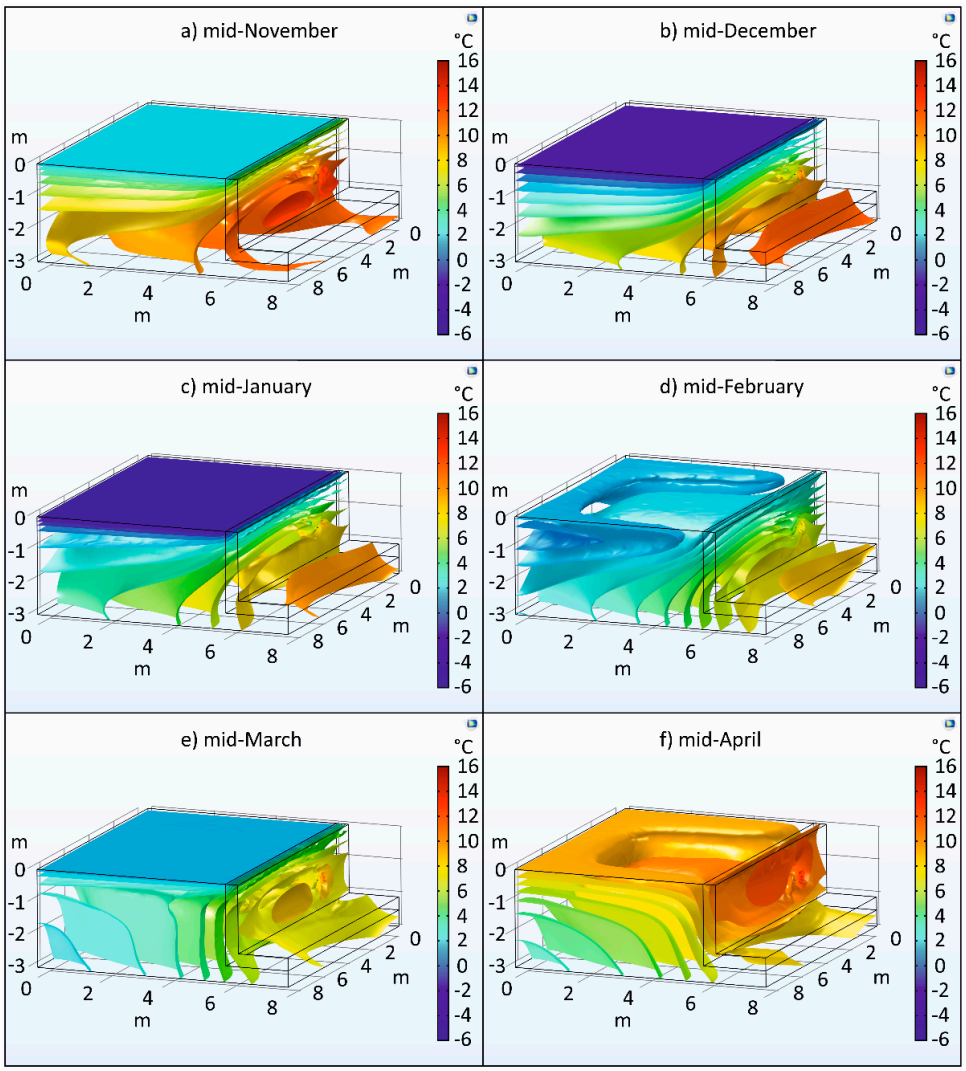

Figure 6. The tri-dimensional temperature isosurfaces for the simulation case 2—HGHE with a heated basement: (**a**) mid-November; (**b**) mid-December; (**c**) mid-January; (**d**) mid-February; (**e**) mid-March; (**f**) mid-April.

The second simulation case can also be considered as an application for residential buildings. Although, not as common as in the first case, some buildings have heated basements. The simulation results indicate that the ground freezing period was reduced by approximately 2–3 weeks compared with the first case simulation. Thus, common

sense implies placing the HGHE near a heated part of the basement in a building where the basement wall and slab are not insulated. This situation can apply to older existing buildings that have basements but aren't properly insulated.

3.3. Case 3: HGHE with Heat from Solar Thermal Panels

In this simulation case, the basement was considered unheated, meaning a temperature of 10 °C inside for the whole heating season, as was the case in the first simulation. The difference between the third simulation case and the previous two cases is that the heat that was transferred into the HGHE with the solar thermal panels was considered. The data was collected from experimental research. The solar thermal panels were a heat source for the HGHE and the heat was stored inside a water tank. The heat was transferred from the pipes during the periods when the heat pump was offline.

Similarly, with simulation case 1, the basement wall and slab have a constant temperature, indicating that the heat transfer was low. Figures 7 and 8 illustrate the effect of heat transfer from the solar thermal panels. The overall temperature inside the HGHE at pipe depth increased by approximately 3.5–4 °C compared to the first case. Thus, the ground freezing period decreased even further with approximately 2 weeks, reducing the total ground freezing period to under 2 months.

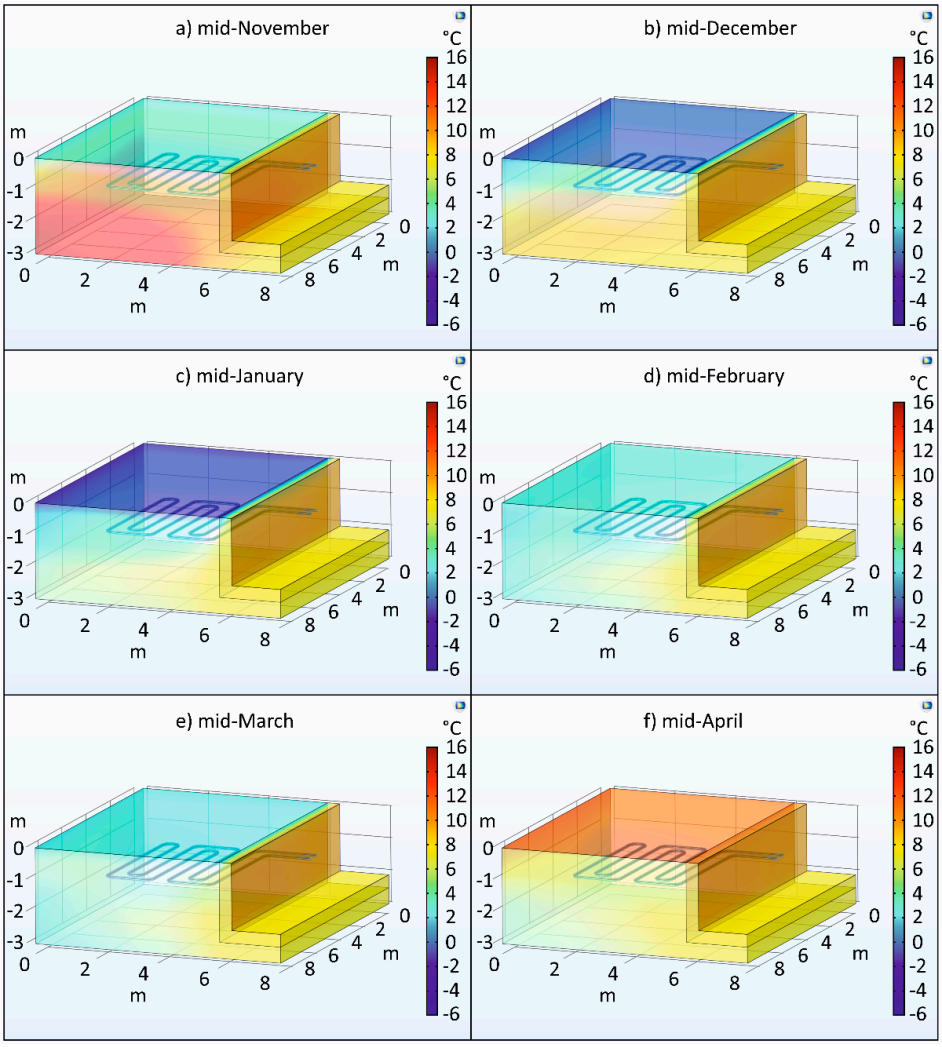

Figure 7. The tri-dimensional temperature gradients for the simulation case 3—HGHE with heat from solar thermal panels: (**a**) mid-November; (**b**) mid-December; (**c**) mid-January; (**d**) mid-February; (**e**) mid-March; (**f**) mid-April.

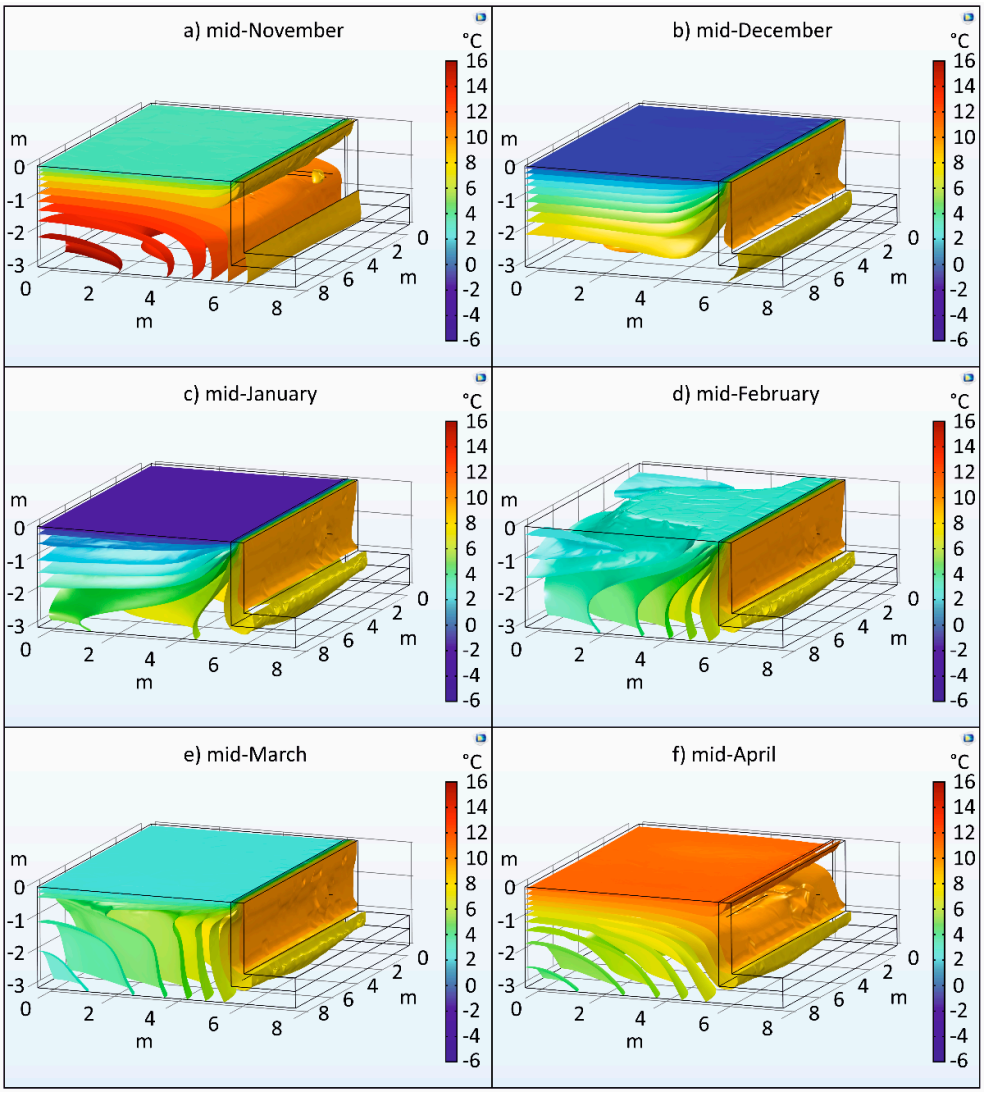

Figure 8. The tri-dimensional temperature isosurfaces for the simulation case 3—HGHE with heat from solar thermal panels: (**a**) mid-November; (**b**) mid-December; (**c**) mid-January; (**d**) mid-February; (**e**) mid-March; (**f**) mid-April.

Interestingly, the overall temperature at pipe depth and in the ground close to the pipes the temperature did not decrease below the freezing point. This did not occur in the second simulation case and it indicates that a higher quantity of heat was transferred inside the HGHE compared with the second simulation case. Moreover, in Figure 8, it can be observed that uniformity with depth occurs most of the heating season. This is explained by the fact that heat is being uniformly transferred from the pipes on a wide area, the whole area created by the HGHE pipes in this case. Even if the unheated basement has a low influence, as the first simulation case indicated, heat transfer inside the HGHE from the solar thermal panels almost negates that effect. This occurs due to the difference in heat quantity from the basement and the solar thermal panels. This can be observed in mid-January and mid-February, where heat distribution layers indicate that heat from the unheated basement is being pushed back inside the basement from the basement slab.

In mid-March and mid-April, because the exterior temperature starts to increase, the ground where the HGHE is placed has a higher overall temperature than the surroundings. This occurs due to the fact that in this period, the heat pump downtime is a lot higher, the temperature difference between the exterior and the interior temperatures is a lot lower, and there is more heat produced with the solar thermal panels. All this indicates that a

high quantity of heat is being transferred inside the HGHE, but also that heat is being lost to the exterior environment. This also occurs in September and October based on the same exterior conditions.

3.4. Case 4: HGHE with Heat from Heated Basement and Solar Thermal Panels Combined

Forth simulation case represents the combination of the second and third simulation cases where both auxiliary heat sources were considered. As expected, the overall ground temperature increased by approximately 5–6 °C. Due to the effect of the heat transfer, the ground freezing period decreased to approximately 1 month. The temperature at pipe depth only decreased at 3 °C in this case. In Figure 9, it can be observed that compared with the third simulation case, the heated basement has a more pronounced impact. This is indicated by the non-uniformity of heat distribution layers by the depth and it is most visible for the season peak. This effect occurs because, in the season peak, the solar thermal panels have the lowest efficiency due to the lowest daytime and cloudiness factor. Meanwhile, the basement heat level is constant. This indicates that the basement heat flux is similar to or possibly higher in the season peak than the heat flux from the solar thermal panels.

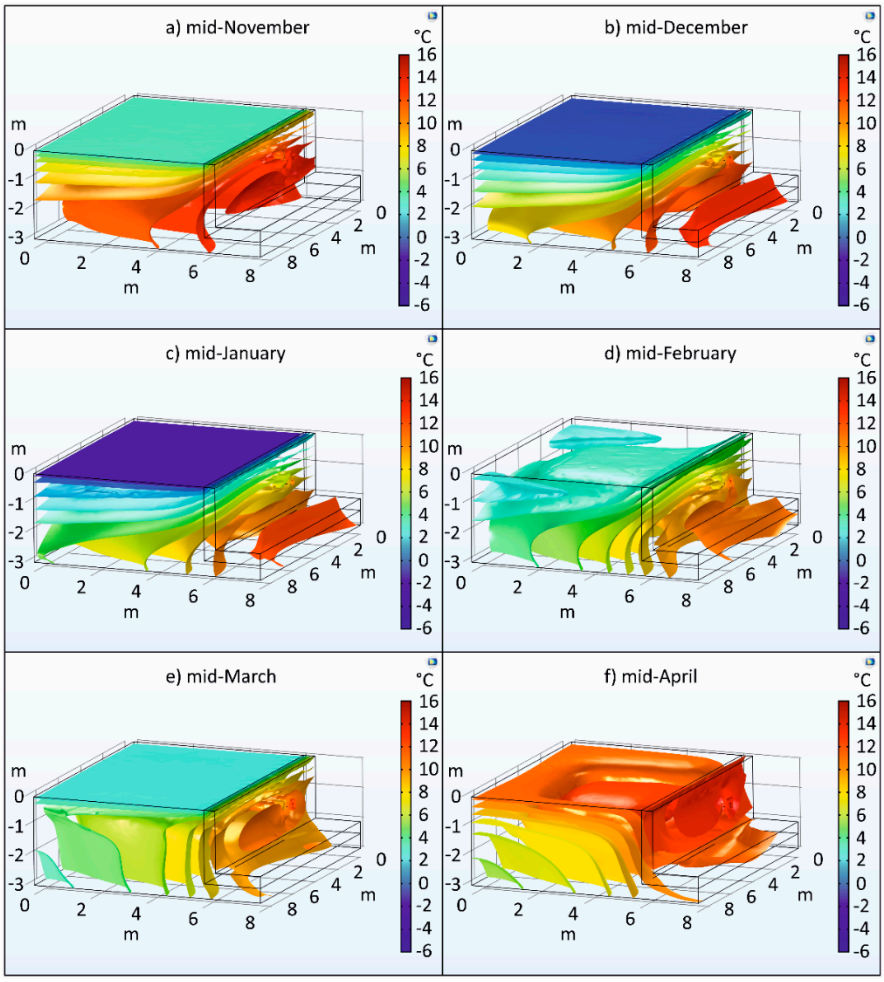

Figure 9. The tri-dimensional temperature isosurfaces for the simulation case 4—HGHE with heated basement and solar thermal panels: (**a**) mid-November; (**b**) mid-December; (**c**) mid-January; (**d**) mid-February; (**e**) mid-March; (**f**) mid-April.

Overall, Figure 9 illustrates the effects of both auxiliary heat sources contributing to the heat balance inside the HGHE. The overall ground temperature resulted in the highest from all four simulation cases, as was expected. Both heat sources combined offer more reliability for the HGHE as a heat source for the heat pump and a more sustainable heat

reservoir during the heating season. These results are only interpreted for an HGHE that works only for the heating season. When the cooling season is considered, results may differ from one season to another and is a subject for another research.

4. Discussion

Based on the results in Section 3, the effects of using auxiliary heat sources for the HGHE are discussed in detail in this chapter.

According to the simulated cases, increasing the overall heat transferred into the HGHE increases the overall temperature inside the HGHE. This, in turn, creates a more sustainable heat reservoir for the heat pump to use to extract heat during the heating season. This effect is observed in Figures 3–9 above and also in Figure 10. Figure 10 illustrates the heat transfer in sections of the HGHE perpendicular to the basement wall, for all 4 cases, for the day that the temperature decreased the most, corresponding to the day of 27 January. This day occurred to be 27 January for this study due to the exterior temperature data used, but it can differ from case to case. Although, the coldest day will presumably always be in the heating season peak. Here, the effect of each auxiliary heat source and the combination between them can be seen, especially regarding the lowest temperature. The lowest temperature increases by approximately 1.5 °C from case 1 to case 2, by approximately 0.5 °C from case 2 to case 3, and by approximately 1 °C from case 3 to case 4. This adds up to an increase of 3 °C between case 1 and case 4 for the coldest day of the heating season.

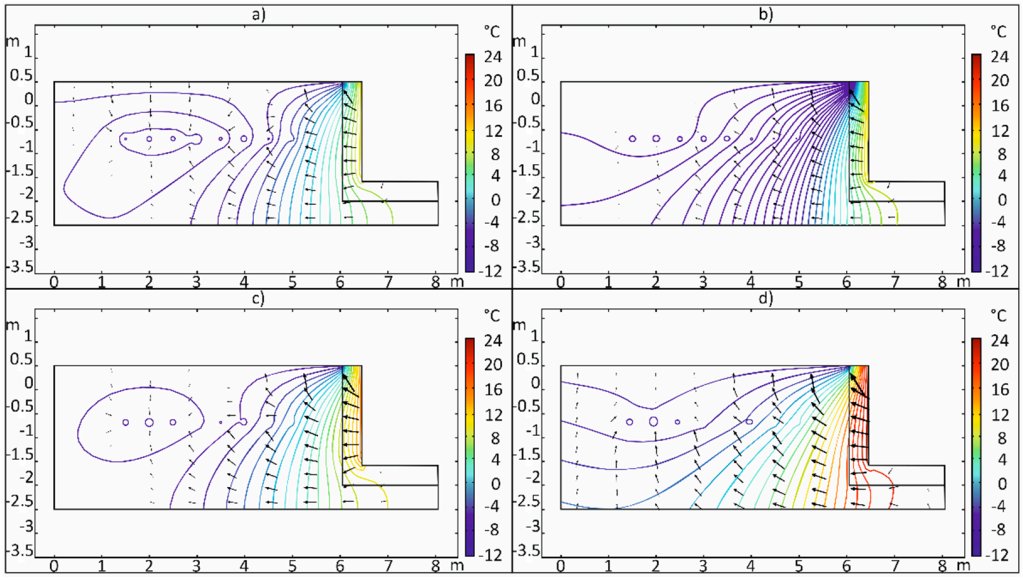

Figure 10. Bi-dimensional section through the HGHE, perpendicular to the basement wall for the day with the lowest temperature simulated, corresponding to the day of 27 January, as follows: (**a**) case 1–no auxiliary heat sources; (**b**) case 2–heated basement; (**c**) case 3–solar thermal panels; (**d**) case 4–both auxiliary heat sources. The arrows indicate the heat direction.

This indicates that with the use of external auxiliary heat sources, the overall temperature inside the HGHE is maintained at higher values, increasing the efficiency of the heat pump and reducing the overall ground temperature variation. HGHEs are influenced by seasonal temperature variation, but the daily temperature variation contributes to the heat pump efficiency decrease also, especially because when the temperature is the lowest, during the night, the heat load needed is the highest.

Table 3 presents the temperatures at pipe depth for the middle of each month of the heating season, corresponding to Figures 3–9. These temperatures represent the mean temperature for the overall surface where the HGHE pipes are buried. The temperature at pipe depth for each simulated case starts at the same value of 12.45 °C. At the end

of the heating season, though, there is a considerable difference between the ground temperatures for the simulated cases and that indicates the positive effect that the auxiliary heat sources had.

Table 3. Temperature at pipe depth.

Corresponding Day	Case 1 [°C]	Case 2 [°C]	Case 3 [°C]	Case 4 [°C]
Mid-October	12.45	12.45	12.45	12.45
Mid-November	7.68	8.41	8.73	8.93
Mid-December	2.19	3.49	4.41	5.20
Mid-January	−2.10	−0.80	1.12	2.91
Mid-February	1.38	2.37	3.59	4.69
Mid-March	4.63	5.33	6.35	7.24
Mid-April	6.49	6.98	8.50	9.10

For the first two simulation cases, it can be observed that the temperatures in mid-January were below the freezing point, but for simulation case 3 and simulation case 4, the temperature did not decrease below zero. This corresponds with the fact that extracting heat with HGHE increases the ground freezing depth for the area where the HGHE pipes are positioned. It indicates that transferring heat into the HGHE prevents ground freezing at pipe depth from occurring. This suggests that in those situations, using a solution of water mixed with ethylene glycol is not necessary for the entire duration of the heating season.

Consequently, transferring heat from auxiliary heat sources into the ground where the HGHE is positioned decreases the ground freezing period, as illustrated in Figures 3–9. The ground freezing period considered represents the period when the ground froze below the normal freezing depth of 0.9 m for the location in Brașov, Romania, where the experimental data was registered. Table 4 presents the starting and ending dates for the freezing periods in concordance with the freezing depth and the total number of days when the ground was frozen. This means that for case 1, with no auxiliary heat sources, between the 21 November and 25 February the ground froze below 0.9 m and reached a maximum depth of approximately 1.4 m.

Table 4. Ground freezing period.

Case	Start	End	Days	Freeze Depth
1–no auxiliary heat source	21 November	25 February	97	~1.40 m
2–heated basement	6 December	16 February	73	~1.20 m
3–solar thermal panels	10 December	5 February	58	~1.13 m
4–both auxiliary heat sources	14 December	18 January	36	~0.92 m

Thus, compared with simulation case 1, the ground freezing period decreased by approximately 24.74% by having a heated basement, approximately 40.20% by transferring heat with solar thermal panels, and approximately 62.88% by using both auxiliary heat sources. This is also observed in Figure 11, where the mean temperature at a pipe depth of 1.2 m is illustrated for all 4 simulation cases in relation to the undisturbed ground temperature measured at a 15 m distance near an unheated part of the basement.

The mean temperature illustrated in Figure 11 represents an average temperature of the 25 m^2 HGHE surface at the pipe depth of 1.2 m. The undisturbed ground temperature is also measured at 1.2 m depth and at a distance of 3.5 m from the basement wall. This corresponds with the distance from the HGHE center to the basement wall.

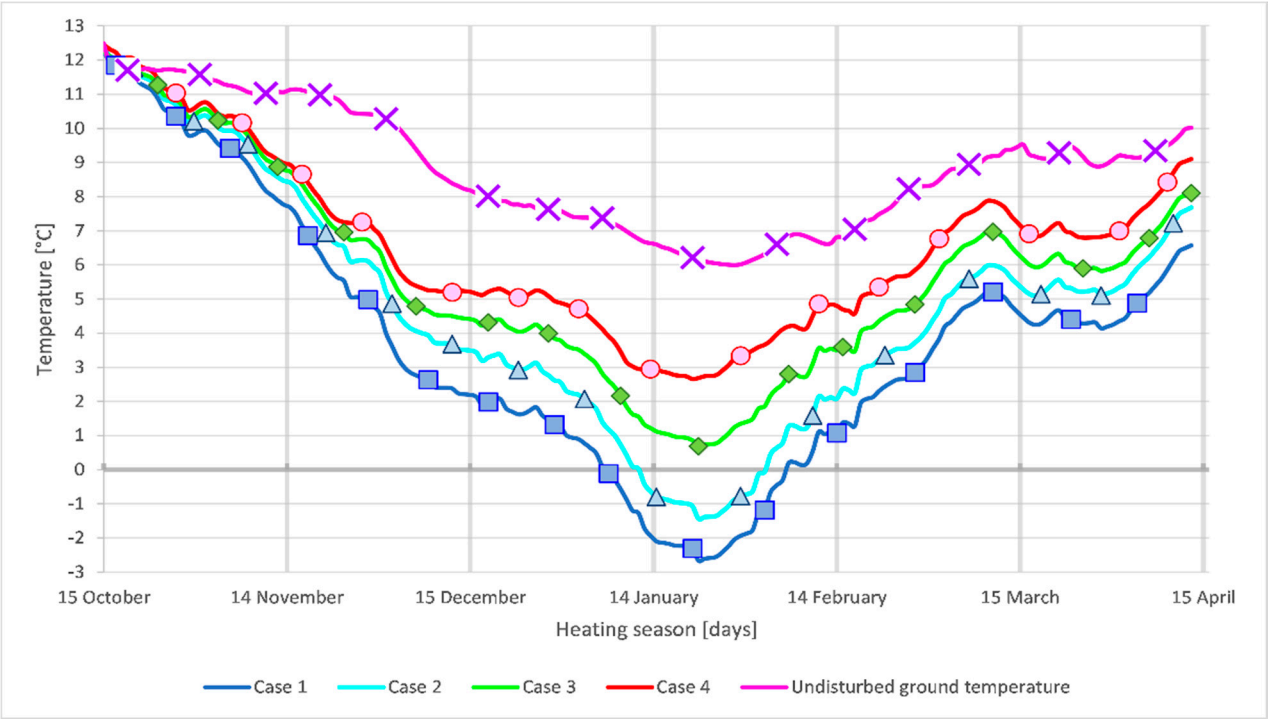

Figure 11. Mean temperature at pipe depth of 1.2 m for HGHE for each simulation case in relation to the measured undisturbed ground temperature.

As observed in Figure 11, the overall mean temperature at pipe depth for all simulation cases starts at 12.45 °C. As time passes, the ground temperature decreases further and further. It indicates that there is a considerable difference between a heated basement (case 2) and heat transfer from thermal solar panels (case 3) compared with no auxiliary heat sources from case 1. There is, though, a benefit of positioning the HGHE near the heated basement, as the mean temperature is approximately 1 °C higher in case 2 than in case 1 almost all season long. At the season peak, auxiliary heat sources are most impactful, the temperature difference being the highest of the season and increasing with more heat that is transferred into the HGHE. After that, for the second part of the season, heat transfer into the HGHE contribute to re-establishing the heat reservoir in the ground where the HGHE is positioned. The difference between the undisturbed ground temperature and the temperature from case 1, with no auxiliary heat sources at the end of the season, is approximate 3.45 °C. On the other end, the difference between the undisturbed ground temperature and the temperature from case 4, with all auxiliary heat sources, is approximately 0.92 °C, which is under 1 °C. Considering all of the above, results indicate that the case 1 ground temperature at the end of the season increases by approximately 2.53 °C, as observed in case 4, by using auxiliary heat sources for transferring heat into the HGHE.

Another important observation is that when the basement is heated, it loses heat, especially on the upper side of the wall, near the exterior air. This can be observed in Figure 5 for the second simulated case, but it occurs for the fourth simulated case also. This effect can be mitigated by insulating the basement wall up to the depth of the pipe with the purpose of directing the basement heat flux through the HGHE pipes. It should be considered for further research.

Auxiliary heat sources have a positive impact on maintaining a higher mean temperature inside the HGHE, thus reducing the negative effects of high-temperature variation at the ground surface. Further research needs to be investigated for alternative solutions regarding auxiliary heat sources. Possible solutions that should be considered are positioning the HGHE under the building or in the ground inside the building foundation, positioning the HGHE near high-temperature rooms, such as thermal plants rooms, laundry cleaning

and drying rooms, industrial kitchens, that are all underground, or any other solution that involves using the residual heat in any way. This research can also be extended for cooling applications with the purpose of removing heat from the HGHE in the cooling season. Possible solutions for this that can be considered are using flat solar panels used to transfer heat from the ground to the exterior air during the night, transferring the heat into domestic hot water tanks or exterior pools, or any other application that requires heat during the cooling season. The main disadvantage of HGHEs is the installation surface needed. Auxiliary heat sources can be used with the purpose of reducing the HGHE area instead of increasing the overall ground temperature and represents a possible direction for further research.

5. Conclusions

This study concentrated on the effect of auxiliary heat sources on the overall temperature inside HGHEs. A numerical model for an HGHE was established that was validated with experimental data [34]. The main conclusions of this research can be summarized as follows:

- Heat transfer inside the HGHE from auxiliary heat sources increases the overall HGHE temperature at the end of the heating season, with 1.11 °C for case 2 (heated basement), 1.53 °C for case 3 (solar thermal panels), 2.53 °C for case 4 (both auxiliary heat sources).
- The ground freezing period decreased by 24.74% in the case of a heated basement, 40.20% by transferring heat inside the HGHE from thermal solar panels, and 62.88% by using both auxiliary sources combined.
- At pipe depth (1.2 m) in case 1, without auxiliary heat sources, the ground froze for 30 days, and for case 2, with a heated basement, the ground froze for 21 days. This indicates that by only positioning the HGHE near a heated basement, the freezing period at pipe depth can decrease by approximately 30%.
- With the use of auxiliary heat sources, the mean temperature at pipe depth can stop the temperature decrease under the freezing point for the entire heating season. In this study, for cases 3 and 4, the ground at a pipe depth of 1.2 m did not freeze for the entire duration of 181 days of the heating season.
- Transferring heat inside the HGHE contributes to stabilizing the overall temperature inside the HGHE heat reservoir for the duration of the heating season, thus reducing the negative effects that exterior temperature variation has on the ground at the surface.
- Due to the extreme variation of daily and seasonal exterior temperature, some quantity of heat from the heat transferred inside the HGHE is lost to the environment, from the ground surface to the exterior air. Residual heat is lost all the time, so smart positioning of the HGHE near residual auxiliary heat sources, such as heated basements, needs to be considered when designing heat pump systems using HGHEs.

Author Contributions: Conceptualization, A.-M.B., G.N. and A.-I.B.; methodology, A.-M.B., G.D. and C.P.; software, A.-I.B., S.-I.B. and N.-F.I.; validation, G.D. and G.N.; formal analysis, V.C. and M.F.; investigation, C.E.C. and O.D.; resources, N.-F.I.; data curation, C.E.C. and O.D.; writing—original draft preparation, A.-M.B.; writing—review and editing, N.-F.I., G.N. and S.-I.B.; visualization, A.-M.B. and C.P.; supervision, V.C. and M.F.; project administration, G.N. and G.D. All authors have read and agreed to the published version of the manuscript.

Funding: This research received no external funding.

Institutional Review Board Statement: Not applicable.

Informed Consent Statement: Not applicable.

Data Availability Statement: The data presented in this study are available on request from the corresponding author. The data are not publicly available due to privacy issues.

Conflicts of Interest: The authors declare no conflict of interest.

References

1. Soeder, D.J. Fossil Fuels and Climate Change BT. In *Fracking and the Environment: A Scientific Assessment of the Environmental Risks from Hydraulic Fracturing and Fossil Fuels*; Soeder, D.J., Ed.; Springer: Berlin/Heidelberg, Germany, 2021; pp. 155–185, ISBN 978-3-030-59121-2.
2. Mann, M.E. Climate Change—False Hope. *Sci. Am.* **2014**, *310*, 78–81. [CrossRef] [PubMed]
3. Lelieveld, J.; Klingmüller, K.; Pozzer, A.; Burnett, R.T.; Haines, A.; Ramanathan, V. Effects of Fossil Fuel and Total Anthropogenic Emission Removal on Public Health and Climate. *Proc. Natl. Acad. Sci. USA* **2019**, *116*, 7192–7197. [CrossRef] [PubMed]
4. Bahmani, M.H.; Hakkaki-Fard, A. A Hybrid Analytical-Numerical Model for Predicting the Performance of the Horizontal Ground Heat Exchangers. *Geothermics* **2022**, *101*, 102369. [CrossRef]
5. Sangi, R.; Müller, D. Dynamic Modelling and Simulation of a Slinky-Coil Horizontal Ground Heat Exchanger Using Modelica. *J. Build. Eng.* **2018**, *16*, 159–168. [CrossRef]
6. Hou, G.; Taherian, H.; Song, Y.; Jiang, W.; Chen, D. A Systematic Review on Optimal Analysis of Horizontal Heat Exchangers in Ground Source Heat Pump Systems. *Renew. Sustain. Energy Rev.* **2022**, *154*, 111830. [CrossRef]
7. Habibi, M.; Amadeh, A.; Hakkaki-Fard, A. A Numerical Study on Utilizing Horizontal Flat-Panel Ground Heat Exchangers in Ground-Coupled Heat Pumps. *Renew. Energy* **2020**, *147*, 996–1010. [CrossRef]
8. Gan, G. A Numerical Methodology for Comprehensive Assessment of the Dynamic Thermal Performance of Horizontal Ground Heat Exchangers. *Therm. Sci. Eng. Prog.* **2019**, *11*, 365–379. [CrossRef]
9. Self, S.J.; Reddy, B.V.; Rosen, M.A. Geothermal Heat Pump Systems: Status Review and Comparison with Other Heating Options. *Appl. Energy* **2013**, *101*, 341–348. [CrossRef]
10. Shi, Y.; Xu, F.; Li, X.; Lei, Z.; Cui, Q.; Zhang, Y. Comparison of Influence Factors on Horizontal Ground Heat Exchanger Performance through Numerical Simulation and Gray Correlation Analysis. *Appl. Therm. Eng.* **2022**, *213*, 118756. [CrossRef]
11. Tang, F.; Lahoori, M.; Nowamooz, H.; Rosin-Paumier, S.; Masrouri, F. A Numerical Study into Effects of Soil Compaction and Heat Storage on Thermal Performance of a Horizontal Ground Heat Exchanger. *Renew. Energy* **2021**, *172*, 740–752. [CrossRef]
12. Yang, W.; Xu, R.; Wang, F.; Chen, S. Experimental and Numerical Investigations on the Thermal Performance of a Horizontal Spiral-Coil Ground Heat Exchanger. *Renew. Energy* **2020**, *147*, 979–995. [CrossRef]
13. Dinh, B.H.; Kim, Y.S.; Yoon, S. Experimental and Numerical Studies on the Performance of Horizontal U-Type and Spiral-Coil-Type Ground Heat Exchangers Considering Economic Aspects. *Renew. Energy* **2022**, *186*, 505–516. [CrossRef]
14. Wu, Y.; Gan, G.; Verhoef, A.; Vidale, P.L.; Gonzalez, R.G. Experimental Measurement and Numerical Simulation of Horizontal-Coupled Slinky Ground Source Heat Exchangers. *Appl. Therm. Eng.* **2010**, *30*, 2574–2583. [CrossRef]
15. Zhou, Y.; Bidarmaghz, A.; Makasis, N.; Narsilio, G. Ground-Source Heat Pump Systems: The Effects of Variable Trench Separations and Pipe Configurations in Horizontal Ground Heat Exchangers. *Energies* **2021**, *14*, 3919. [CrossRef]
16. Fujii, H.; Yamasaki, S.; Maehara, T.; Ishikami, T.; Chou, N. Numerical Simulation and Sensitivity Study of Double-Layer Slinky-Coil Horizontal Ground Heat Exchangers. *Geothermics* **2013**, *47*, 61–68. [CrossRef]
17. Selamat, S.; Miyara, A.; Kariya, K. Numerical Study of Horizontal Ground Heat Exchangers for Design Optimization. *Renew. Energy* **2016**, *95*, 561–573. [CrossRef]
18. Tang, F.; Nowamooz, H. Outlet Temperatures of a Slinky-Type Horizontal Ground Heat Exchanger with the Atmosphere-Soil Interaction. *Renew. Energy* **2020**, *146*, 705–718. [CrossRef]
19. Pu, L.; Xu, L.; Qi, D.; Li, Y. Structure Optimization for Horizontal Ground Heat Exchanger. *Appl. Therm. Eng.* **2018**, *136*, 131–140. [CrossRef]
20. Ariwibowo, T.H.; Miyara, A. Thermal Characteristics of Slinky-Coil Ground Heat Exchanger with Discrete Double Inclined Ribs. *Resources* **2020**, *9*, 105. [CrossRef]
21. Liu, X.; Li, C.; Zhang, G.; Zhang, L.; Wei, B. Numerical Investigation on Energy Efficiency of Heat Pump with Tunnel Lining Ground Heat Exchangers under Building Cooling. *Buildings* **2021**, *11*, 661. [CrossRef]
22. Sterpi, D.; Tomaselli, G.; Angelotti, A. Energy Performance of Ground Heat Exchangers Embedded in Diaphragm Walls: Field Observations and Optimization by Numerical Modelling. *Renew. Energy* **2020**, *147*, 2748–2760. [CrossRef]
23. Nam, Y.; Chae, H. Numerical Simulation for the Optimum Design of Ground Source Heat Pump System Using Building Foundation as Horizontal Heat Exchanger. *Energy* **2014**, *73*, 933–942. [CrossRef]
24. Aresti, L.; Christodoulides, P.; Panayiotou, G.P.; Florides, G. Residential Buildings' Foundations as a Ground Heat Exchanger and Comparison among Different Types in a Moderate Climate Country. *Energies* **2020**, *13*, 6287. [CrossRef]
25. Bao, X.; Qi, X.; Cui, H.; Zou, J.; Xiao, X. Comparison Study on the Performance of a Novel and Traditional Energy Piles by Laboratory Tests. *Symmetry* **2021**, *13*, 1958. [CrossRef]
26. Tan, L.; Love, J.A. A Literature Review on Heating of Ventilation Air with Large Diameter Earth Tubes in Cold Climates. *Energies* **2013**, *6*, 3734–3743. [CrossRef]
27. Baglivo, C.; D'Agostino, D.; Congedo, P.M. Design of a Ventilation System Coupled with a Horizontal Air-Ground Heat Exchanger (HAGHE) for a Residential Building in a Warm Climate. *Energies* **2018**, *11*, 2122. [CrossRef]
28. Bonuso, S.; Panico, S.; Baglivo, C.; Mazzeo, D.; Matera, N.; Congedo, P.M.; Oliveti, G. Dynamic Analysis of the Natural and Mechanical Ventilation of a Solar Greenhouse by Coupling Controlled Mechanical Ventilation (CMV) with an Earth-to-Air Heat Exchanger (EAHX). *Energies* **2020**, *13*, 3676. [CrossRef]

29. Baglivo, C.; Bonuso, S.; Congedo, P.M. Performance Analysis of Air Cooled Heat Pump Coupled with Horizontal Air Ground Heat Exchanger in the Mediterranean Climate. *Energies* **2018**, *11*, 2704. [CrossRef]
30. D'Agostino, D.; Esposito, F.; Greco, A.; Masselli, C.; Minichiello, F. The Energy Performances of a Ground-to-Air Heat Exchanger: A Comparison among Köppen Climatic Areas. *Energies* **2020**, *13*, 2895. [CrossRef]
31. Greco, A.; Masselli, C. The Optimization of the Thermal Performances of an Earth to Air Heat Exchanger for an Air Conditioning System: A Numerical Study. *Energies* **2020**, *13*, 6414. [CrossRef]
32. Kupiec, K.; Gwadera, M. Heat Balance of Horizontal Ground Heat Exchangers. *Ecol. Chem. Eng. S* **2018**, *25*, 537–548. [CrossRef]
33. Leski, K.; Luty, P.; Gwadera, M.; Larwa, B. Numerical Analysis of Minimum Ground Temperature for Heat Extraction in Horizontal Ground Heat Exchangers. *Energies* **2021**, *14*, 5487. [CrossRef]
34. Bulmez, A.M.; Ciofoaia, V.; Năstase, G.; Dragomir, G.; Brezeanu, A.I.; Şerban, A. An Experimental Work on the Performance of a Solar-Assisted Ground-Coupled Heat Pump Using a Horizontal Ground Heat Exchanger. *Renew. Energy* **2022**, *183*, 849–865. [CrossRef]